

## Polarization effects in electromagnetically induced transparency

D. McGloin,\* M. H. Dunn, and D. J. Fulton

*J. F. Allen Physics Research Laboratories, Department of Physics and Astronomy, University of St. Andrews, St. Andrews, Fife KY16 9SS, Scotland, United Kingdom*

(Received 22 March 2000; published 10 October 2000)

We demonstrate the magnitude dependence of electromagnetically induced transparency, in a three-level cascade scheme in rubidium, on the probe and coupling field polarizations. We show that this dependence is due to the presence of the degenerate magnetic sublevels and the strengths of their relative dipole matrix elements. It is shown that this can lead to modified absorption profiles when electromagnetically induced transparency is used for spectroscopic purposes. We present theory that is in good agreement with our experiments.

PACS number(s): 42.50.Gy, 42.25.Ja, 32.70.-n

### I. INTRODUCTION

Electromagnetically induced transparency (EIT) [1] is a phenomena in which an atom subjected to a weak probe field on one transition and a stronger coupling field on a linked transition will no longer absorb the probe radiation. As well as being of considerable interest in its own right, EIT underpins phenomena such as lasing without inversion [2] and more recently, slow light [3–5]. In the following paper, we present a study of probe and coupling field polarization on the EIT absorption trace in a multilevel cascade scheme within rubidium. Previously, the role of polarization has been largely ignored in studies of EIT, although of late there has been some interest, particularly in coherent control of polarization [6], where EIT is used to change the polarization state of the probe field, thus turning the atomic medium into a waveplate. Interest has also fallen on the use and enhancement of magneto-optical effects [5,7,8], where EIT effects coupled with nondegenerate magnetic sublevels can produce enhancement of magneto-optical rotation and even produce a magneto-optical switch. Studies by Durrant *et al.* [9] have examined the role of polarization in EIT in a Lambda scheme within a MOT. We also note that a study of polarization effects as a function of beam intensity in two-level systems has been carried out by Lezama *et al.* [10] while both Ling *et al.* [11] and Fulton *et al.* [12] have examined EIT in media with Zeeman structure. A theory of saturation spectroscopy outlined by Feuilleade and Berman [13] may be relevant for this work but is beyond the scope of the simple theoretical outline taken here.

In this paper, we examine the effects of polarization on a system with degenerate magnetic sublevels. Many papers that discuss EIT mention some arbitrary use of coupling field or probe field polarization but never actually discuss why those polarizations were chosen. In this paper, we discuss why it may be appropriate to choose certain polarizations in a typical EIT experiment. It is shown that the Zeeman-level degeneracy is responsible for the changing EIT absorption profiles observed when the polarizations of the optical fields are varied. More specifically, we examine the “two-routes to

excitation” model of EIT and show that the strength of the two-photon absorption results in enhancement or degradation of EIT depending on the probe and coupling field polarization. In our cascade scheme it is also possible to resolve the hyperfine structure of the upper coupling field level using EIT [14], and we show how polarization affects this method of atomic spectroscopy.

### II. THEORETICAL CONSIDERATIONS

#### A. Two-photon effects

The experimental atomic system is shown in Fig. 1. It is in essence a simple three-level cascade scheme used in a number of experiments [15,16]. However, rubidium has a much more complicated structure due to its intrinsic nuclear spin, therefore in order to examine fully the two-photon effects, we must take into account all the sublevels. Note that in this paper we only consider the  $5S_{1/2}(F=2) - 5P_{3/2}(F'=1,2,3) - 5D_{5/2}(F''=1,2,3,4)$  transitions of  $\text{Rb}^{87}$  but our arguments are valid for any of the rubidium isotopes or ground-state  $F$  levels. Previously, the authors have shown the role that two-photon interference plays in EIT [14]. Extending this work by calculating the two-photon transition probabilities for the  $5S_{1/2} - 5P_{3/2} - 5D_{5/2}$  transition, we are able to predict the relative magnitudes of EIT features for various probe and coupling field polarization orientations. The transition amplitude for an atomic transition between two  $m_F$  levels is given by [17]

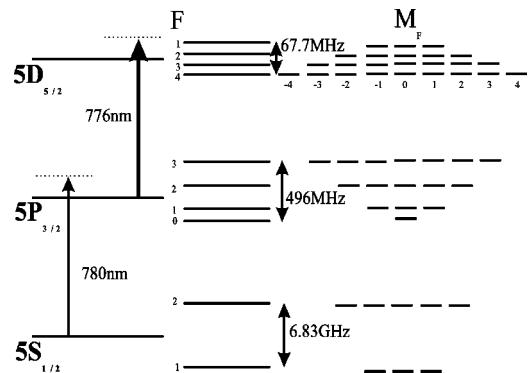


FIG. 1. The atomic system under consideration:  $\text{Rb}^{87}(5S_{1/2} - 5P_{3/2} - 5D_{5/2})$ .

\*FAX: +44 (0)1334 463104. Email address: dm11@st-and.ac.uk

$$\begin{aligned}
& \langle IJFm_F | d_q | I'J'F'm'_F \rangle \\
& = (-1)^{F-m_F} \begin{pmatrix} F & 1 & F' \\ -m_F & q & m'_F \end{pmatrix} \\
& \quad \times (-1)^{I+J+F+1} \sqrt{(2F+1)(2F'+1)} \\
& \quad \times \begin{Bmatrix} J & 1 & J' \\ F' & 1 & F \end{Bmatrix} (J \| d \| J'), \quad (1)
\end{aligned}$$

where  $I$  is the nuclear spin ( $I=3/2$  for Rb<sup>87</sup>),  $J$  is the angular momentum,  $F$  is the total angular momentum, and  $m_F$  stands for the magnetic sublevels of  $F$  states. Each  $F$  state has  $(2F+1)$  degenerate  $m_F$  values. The primes on the quantum numbers (e.g.,  $J'$ ) correspond to the initial state in which the atom resides. The value  $d_q$  is the dipole operator and the value of  $q$  is polarization dependent, with

$$q = m_F - m'_F = 0 \quad (2)$$

for linearly polarized light and

$$q = m_F - m'_F = \pm 1 \quad (3)$$

for circularly polarized light. The value  $(J \| d \| J')$  is the reduced matrix element as defined by Shore [17], and can be left unevaluated if one is considering only the relative dipole matrix strengths, as is the case in this work. The values in the parentheses denote standard 3j symbol notation and similarly, the values in the curly brackets denote standard 6j symbols [17,18]. In this work they are evaluated via a mathematical algebra package.

We can then easily calculate the relative transition strengths [without evaluating the reduced matrix element  $(J \| d \| J')$ ] using

$$S_q = |\langle IJFm_F | d_q | IJ'F'm'_F \rangle|^2. \quad (4)$$

We then normalize the relative transition strengths for each transition for given initial values of  $F$  and  $q$  (polarization). The normalized transition strengths are then treated as the probability value for excitation, and by appropriate addition and multiplication we are able to calculate the probability of starting in a given  $F$ ,  $m_F$  level and ending up in any other  $F$ ,  $m_F$  level. As such we are able to predict values for the two-photon transition strengths and hence the strength of observed EIT features.

In examining the EIT in our cascade system, we use nine combinations of field polarization, with  $\pi$  representing linearly polarized light;  $\sigma^+$ , right-handed circularly polarized light and  $\sigma^-$ , left-handed circularly polarized light. We see that there are a number of possible transition routes to the upper state, each with its own weighted probability. By multiplying probabilities for the two transitions ( $5S_{1/2} - 5P_{3/2}$ ) and ( $5P_{3/2} - 5D_{5/2}$ ), we end up with a two-photon transition probability for each allowed  $m_F$  to  $m_F$  level. Then, summing over all allowed transitions, we arrive at a transition probability between  $F$  states. The full set of probabilities can be seen in Table I below. The values for the case where both

TABLE I. Transition probabilities for atoms moving between the  $5S_{1/2}(F=2) - 5P_{3/2}(F'=1,2,3) - 5D_{5/2}(F''=1,2,3,4)$  states as parts of 35 000, for each possible polarization geometry.

Probe polarization	Coupling polarization	Peak I $F''=4$	Peak II $F''=3$	Peak III $F''=2$	Peak IV $F''=1$
$\pi$	$\pi$	3600	1232	1160	168
$\pi$	$\sigma^+$	2700	2044	695	231
$\pi$	$\sigma^-$	2700	2044	695	231
$\sigma^+$	$\sigma^+$	5400	1848	690	252
$\sigma^+$	$\sigma^-$	900	1428	1165	147
$\sigma^+$	$\pi$	2700	2044	695	231
$\sigma^-$	$\sigma^-$	5400	1848	690	252
$\sigma^-$	$\sigma^+$	900	1428	1165	147
$\sigma^-$	$\pi$	2700	2044	695	231

optical fields have  $\pi$  polarization have been included in Fig. 2.

It should be noted that for our system we can legitimately multiply and add across the relevant dipole transitions because each system is independent of the others. An examination of Fig. 2 highlights this fact. In order to end up in the  $5D_{5/2}(F=1)$  upper state, an atom may interact with the applied optical fields and arrive in this state via either the  $5P_{3/2}(F=1)$  or  $5P_{3/2}(F=2)$  intermediate state. The choice of which route is employed by the atom is dependent on its relative velocity. This velocity component selects which intermediate level the atom is Doppler shifted into resonance

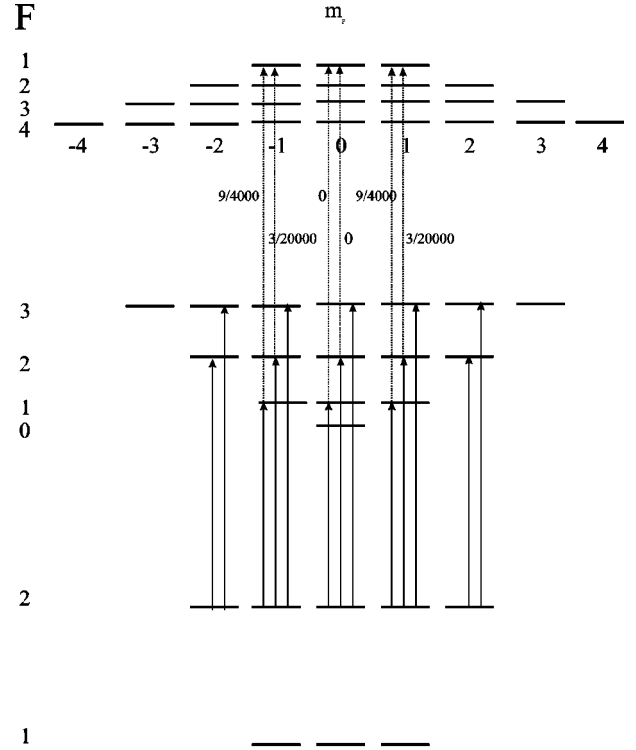


FIG. 2. Possible transitions in the linear-linear polarization case with  $q=0$ . Normalized transition probabilities of allowed two-photon transitions, ending in the  $5D_{5/2}(F=1)$  state are given.

TABLE II. Relative probabilities for getting to the  $5S_{1/2}(F=2) - 5P_{3/2}(F'=1,2,3) - 5D_{5/2}(F''=4)$  state, normalized to the largest value for each polarization orientation. This value gives a value of the relative amount of EIT found for a pair of given polarizations.

Probe polarization	Coupling polarization	Peak I
$\pi$	$\pi$	0.69
$\pi$	$\sigma^+$	0.48
$\pi$	$\sigma^-$	0.45
$\sigma^+$	$\sigma^+$	1
$\sigma^+$	$\sigma^-$	0.16
$\sigma^+$	$\pi$	0.48
$\sigma^-$	$\sigma^-$	0.97
$\sigma^-$	$\sigma^+$	0.16
$\sigma^-$	$\pi$	0.51

with, and hence which route it employs to the upper level. If the situation had been that the atom had a certain probability of employing one route as opposed to the other then the route to the upper state would be more complicated. It would involve calculating the coherent superposition of two separate wave functions and therefore we would be unable to simply add and multiply across the normalized transition probabilities.

Shown in Table II are the two-photon transition probabilities of ending up in the  $F=4$  state of the  $5D_{5/2}$  level, normalized against the largest value. This gives us a measure of the relative amount of EIT we expect for each combination of field polarizations.

### B. Observation of Doppler-free EIT

To conclude our theory section, we briefly look at the conditions for observing sub-Doppler EIT. EIT is a two-photon resonance process [14]. The location of an EIT resonance in the cascade system is given by

$$\Delta_1 + \Delta_2 = 0, \quad (5)$$

where  $\Delta_1$  is the probe field detuning (Fig. 1), and  $\Delta_2$ , the coupling field detuning. Therefore, the location of an EIT resonance is independent of the structure and position of the intermediate level. It is the energy separation of the lower and upper levels, relative to the photon energies of the applied optical fields that is the important parameter. However, for the EIT effect to be physically observed it is required that the probe field falls within the absorption linewidth of the  $5S_{1/2} - 5P_{3/2}$  probe transition. The individual detunings can be written in terms of the Doppler shift  $kV_z$  on a transition for an atom with velocity component  $V_z$  in the direction of the beam propagation:

$$\Delta_1 = \Delta_1^0 + k_1 V_z, \quad (6)$$

$$\Delta_2 = \Delta_2^0 + k_2 V_z, \quad (7)$$

where  $\Delta_i^0$  is the detuning of the applied field from the atomic transition and  $k_i$  is the wave number of the applied light. In order to observe sub-Doppler effects on the probe field it is

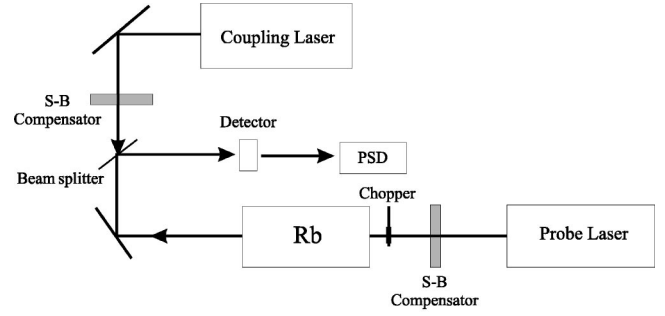


FIG. 3. Experimental setup.

necessary to reduce the two photon residual linewidth below that of the single photon probe field Doppler width. The residual Doppler width of the two-photon transition is

$$\Delta \nu_D = |(k_1 + k_2)u|, \quad (8)$$

where

$$u = \sqrt{\frac{2k_B T}{M}}, \quad (9)$$

$T$  being the temperature of the gas and  $M$  the atomic mass. The first requirement to minimize the residual Doppler width is to choose a system that employs optical fields of nearly equal wavelengths, i.e.,  $|k_1| \approx |k_2|$ . If the two input fields then counterpropagate, the frequency shifts on the individual transitions will be in the opposite direction and the residual Doppler width will be low, similar to the situation occurring in Doppler-free, two-photon spectroscopy [19]. For the cascade system being considered in this work, the copropagating two-photon width is 536 MHz, while with counterpropagating fields this value reduces to only 1.38 MHz, at 320 K. These values compare with the single-photon probe Doppler width of 528 MHz. Therefore, the fact that the probe and coupling field wavelengths are closely matched can be used, in effect, to cancel out the masking effects of Doppler broadening on the probe transition that would normally act to obscure the observation of EIT.

### III. EXPERIMENTAL SETUP

The experimental setup used to investigate these effects is shown in Fig. 3. We make use of two single frequency continuous wave Ti:sapphire lasers, one being a Microlase MBR-110 that is employed as the probe field. It generates light at around 780 nm for interaction with the  $5S_{1/2} - 5P_{3/2}$  transition and is tuneable across this atomic transition. It has a linewidth of  $<100$  kHz. The coupling laser is a modified Schwarz Electro-Optic Titan CW and provides radiation at around 776 nm for interaction with the  $5P_{3/2} - 5D_{5/2}$  transition. The coupling laser is passively stable and it is possible to manually tune it by employing a solid etalon and a set of Brewster plates. It has a linewidth of  $<5$  MHz. We estimate that the coupling field Rabi frequency is approximately 30 MHz. The rubidium cell used is 2 cm long and is heated to approximately  $60^\circ\text{C}$ . The coupling field is unfocused through the cell and the probe is only weakly

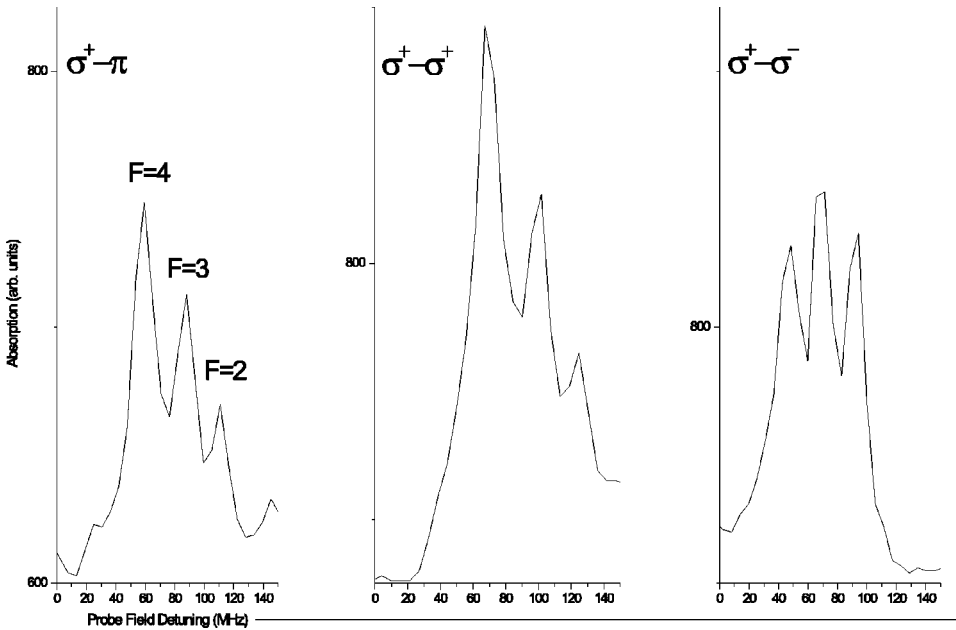


FIG. 4. Experimental traces: (a)  $\sigma^+ - \pi$  (b)  $\sigma^+ - \sigma^+$  (c)  $\sigma^+ - \sigma^-$ .

focused in order to keep its spatial profile within that of the coupling field. We do not employ further focusing of the beams so as to minimize power-broadening effects. The absorption traces are monitored by a photodiode placed after the cell- and phase-sensitive detection is used to improve the signal-to-noise ratio. In order to control the polarization of the fields, a Soleil-Babinet compensator is placed in the path of both the probe and coupling fields before they enter the cell. Both fields are linearly polarized in the same sense before propagation through the compensators. It should be noted that if the polarization of the probe and coupling field are set to be in the same circular polarization, then the atomic sample will “observe” the polarization of both fields as though they are circularly polarized in the opposite sense since the beams are counterpropagating.

IV. EXPERIMENTAL RESULTS

The experimental traces corresponding to the rows VI, IV and V of Table I have been reproduced in Figs. 4(a), (b), and (c), respectively. It can be seen that each of the absorption profiles are broadly similar, each consisting of three resolvable EIT peaks. In all the traces there should in fact be a fourth peak, corresponding to the  $F=1$  state in the  $5D_{5/2}$  level, however the relative dipole strengths of the two-photon routes terminating in this state are so weak that these peaks cannot be resolved. The relative depths of each of these peaks can be seen to depend on the relative polarization orientations of the applied optical field as predicted. Figure 5 compares directly the situation outlined in rows IV and V of Table I. It can clearly be seen that the depth of the EIT feature in the  $\sigma^+ - \sigma^+$  case is much greater than in the  $\sigma^+ - \sigma^-$  case.

V. DISCUSSION

In general EIT experiments upper-state hyperfine structure would not be observed due to power-broadening effects.

This is due to the fact that high-powered coupling fields are normally employed and both fields are also usually focused within the cell in order to obtain better spatial profile matching of the beams. The combined effect is to induce coupling field Rabi frequencies much closer to the single-photon Doppler width of the probe field (i.e.,  $\gg \Delta \nu_D$ ) and hence power-broadening effects become significant. In this experiment, by choosing not to focus the optical fields, we are able to resolve the hyperfine levels in the upper transition as shown in the experimental traces in Figs. 4 and 5. It is well known that the two-photon absorption route is fundamental to the EIT process. It is the interference between the one- and two-photon routes to the upper probe level that is of fundamental importance in EIT. This has clearly been shown by Moseley *et al.* [14]. Therefore, the greater the probability of a two-photon transition within a particular system, the greater the EIT feature we would expect to observe. Thus as the two-

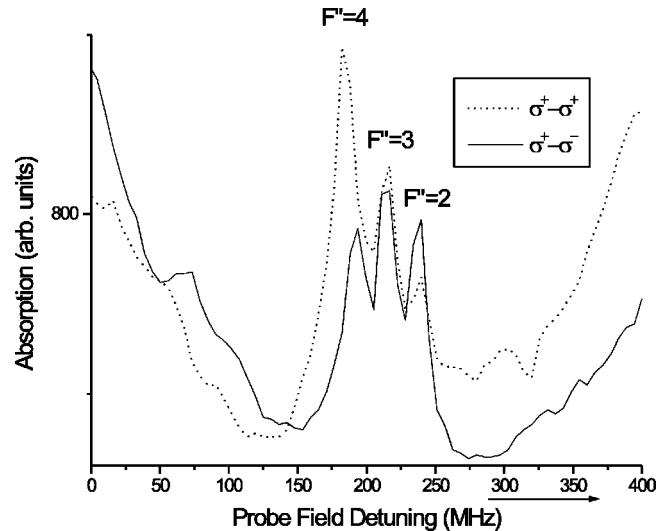


FIG. 5. Change in depth of EIT with polarization. Dashed line corresponds to  $\sigma^+ - \sigma^+$  case, solid line is  $\sigma^+ - \sigma^-$  case.

photon transition probability changes, as it will do as the probe and coupling field are altered, we expect the EIT to change as well. EIT is the imprint of the two-photon process on the probe field absorption. This is exactly what we observe, as outlined in Fig. 5. In the case of  $\sigma^+ - \sigma^+$  polarization, we expect a two-photon probability of 0.22 of being in the  $5D_{5/2}$  level; compare this to the probability of 0.11 of being in the  $5D_{5/2}$  level with  $\sigma^+ - \sigma^-$  polarization. We see in Fig. 4 that the overall amount of EIT does indeed change from one polarization orientation to the next, explained quite simply by the two-photon transition probabilities.

We now examine the EIT traces showing the structure in the upper coupling field level. Consider the three traces shown in Fig. 4. It can be seen that there is a significant difference when the circular polarization of the applied fields is in the same or opposite sense (as experienced by the atomic sample). Relative to the  $\sigma^+ - \sigma^+$  field orientation, it can be seen that in the  $\sigma^+ - \sigma^-$  case the  $F=4$  peak is significantly reduced, to such an extent that the  $F=3$  peak is larger. These results are readily explained when the two-photon probabilities are examined (see Table I). However, we cannot directly compare the EIT in each of the polarization cases. This is due to the fact that rotation of the Soleil-Babinet compensators shifts the probe and coupling beams slightly changing their overlap. Also, the drift of the coupling field changes the exact position of the peaks and hence exactly where their height should be measured from. We can however, examine how our theory compares with experiment in each individual case. In Fig. 4(a), the  $\sigma^+ - \pi$  case, we predict a ratio of peak depths ( $F=4:F=3:F=2$ ) of 1.32:1.0:0.34. We observe a ratio of 1.2:1:0.6, in reasonably good agreement with our predictions. For the  $\sigma^+ - \sigma^+$  case, [Fig. 4(b)], we predict a ratio of 2.92:1:0.37 and observe a ratio of 1.62:1:0.46, which implies we did not resolve the  $F=4$  peak with enough resolution. In the final case of  $\sigma^+ - \sigma^-$ , [Fig. 4(c)], we predict a ratio of 0.63:1:0.82 and predict a slightly worse ratio of 0.83:1:0.88. So our predictions are in broad agreement with our observations and the general trends in relative peak sizes are all correct. We also see from Table I that in fact the optimum orientation for observing EIT is when the field orientations are circularly polarized in the same sense as seen by the atom. The prediction of the two effects whereby the EIT is maximized in the  $\sigma^+ - \sigma^+$

case and the fact that the  $F=4$  hole is larger than the  $F=3$  hole in the  $\sigma^+ - \sigma^-$  case (which is not an obvious result) mean our theory is largely correct.

Such findings have potential use when using EIT as a method of spectroscopy [14]. We can envisage a situation where hyperfine structure is unable to be resolved, for example due to power-broadening effects of the coupling field. If we can change polarization orientation to enhance the EIT, we can bring down the required coupling field power and therefore begin to resolve the structure. We note that such effects in other schemes; e.g., Lambda and V scheme may also be of interest [7].

## VI. CONCLUSIONS

In conclusion, we have shown that the polarization of the optical fields plays an important role in electromagnetically induced transparency experiments. EIT can be enhanced or degraded by the appropriate choice of polarization for the probe and coupling fields. We have shown that this phenomenon is a direct result of the relative probability of the two-photon transition from the ground state to the upper state connected by the coupling field. By taking into account all of the degenerate magnetic hyperfine levels, it was possible to explore and explain the cases where EIT may be used as a method of spectroscopy to examine the hyperfine structure of this upper coupling field state. Again it was seen that polarization orientation effects were evident. EIT absorption profiles can be significantly altered by use of appropriate polarization orientations of the optical fields. If EIT is to be employed as a method of spectroscopy, this must be taken into account. A second area of relevance where these effects should be considered is in experiments to study EIT effects where a magnetic field is applied to a medium in order to lift the magnetic sublevel degeneracy, i.e., in magneto-optical effects.

## ACKNOWLEDGMENTS

The authors wish to thank the Engineering and Physical Sciences Research Council (EPSRC) for research funding under Grant No. GR/L32118. Further, D.M. wishes to acknowledge financial support from the EPSRC.

- 
- [1] J.P. Marangos, *J. Mod. Opt.* **45**, 471 (1998).
  - [2] S.E. Harris, *Phys. Rev. Lett.* **62**, 1033 (1989).
  - [3] L.V. Hau, S.E. Harris, Z. Dutton, and C.H. Behroozi, *Nature (London)* **397**, 594 (1999).
  - [4] M.M. Kash, V.A. Sautenkov, A.S. Zibrov, L. Hollberg, G.R. Welch, M.D. Lukin, Y. Rostovtsev, E.S. Fry, and M.O. Scully, *Phys. Rev. Lett.* **82**, 5229 (1999).
  - [5] D. Budker, D.F. Kimball, S.M. Rochester, and V.V. Yashchuk, *Phys. Rev. Lett.* **83**, 1767 (1999).
  - [6] S. Wielandy and A.L. Gaeta, *Phys. Rev. Lett.* **81**, 3359 (1998).
  - [7] A.K. Patnaik and G.S. Agarwal, e-print, quant-ph/9911034.
  - [8] A.K. Patnaik and G.S. Agarwal, e-print, quant-ph/9908020.
  - [9] A.V. Durrant, H.X. Chen, S.A. Hopkins, and J.A. Vaccaro, *Opt. Commun.* **151**, 136 (1998).
  - [10] A. Lezema, S. Barreiro, A. Lipsich, and A.M. Akulshin, *Phys. Rev. A* **61**, 013801 (1999).
  - [11] H. Y. Ling, Y. Q. Li, and M. Xiao, *Phys. Rev. A* **53**, 1014 (1996).
  - [12] D.J. Fulton, R.R. Moseley, S. Shepherd, B.D. Sinclair, and M.H. Dunn, *Opt. Commun.* **116**, 61 (1995).
  - [13] C. Feuillade and P.R. Berman, *Phys. Rev. A* **29**, 1236 (1984).
  - [14] R.R. Moseley, S. Shepherd, D.J. Fulton, B.D. Sinclair, and M.H. Dunn, *Opt. Commun.* **119**, 61 (1995).
  - [15] D.J. Fulton, S. Shepherd, R.R. Moseley, B.D. Sinclair, and

M.H. Dunn, Phys. Rev. A **52**, 2302 (1995).

[16] S. Jin, Y. Li, and M. Xiao, Opt. Commun. **119**, 90 (1995).

[17] B.W. Shore, *The Theory of Coherent Atomic Excitation* (Wiley, New York, 1990).

[18] M. Weissbluth, *Atoms and Molecules, Student Edition* (Academic Press, London, 1978).

[19] V.S. Letokhov and V.P. Chebotayev, *Nonlinear Laser Spectroscopy* (Springer-Verlag, Berlin, 1977).